

## Vision and visual cortical maps in mice with a photoreceptor synaptopathy: Reduced but robust visual capabilities in the absence of synaptic ribbons

Bianka Goetze<sup>a</sup>, Karl-Friedrich Schmidt<sup>a</sup>, Konrad Lehmann<sup>a</sup>, Wilko Detlev Altmack<sup>b</sup>,  
Eckart Dieter Gundelfinger<sup>b</sup>, Siegrid Löwel<sup>a,\*</sup>

<sup>a</sup> Institut für Allgemeine Zoologie und Tierphysiologie, Erbertstrasse 1, D-07743 Jena, Germany

<sup>b</sup> Leibniz-Institut für Neurobiologie, Abteilung Neurochemie & Molekularbiologie, Brenneckestr. 6, D-39118 Magdeburg, Germany

### ARTICLE INFO

#### Article history:

Received 5 May 2009

Revised 6 October 2009

Accepted 7 October 2009

Available online 22 October 2009

### ABSTRACT

How little neurotransmission in the visual system is sufficient to promote decent visual capabilities? This question is of key importance for therapeutic approaches to restore vision in patients who suffer from degenerative retinal diseases. In the retinae of mice, mutant for the presynaptic scaffolding protein Bassoon (Bsn), signal transfer at photoreceptor ribbon synapses is severely disturbed due to impaired ribbon attachment to the active zone. We have used two different behavioural tasks and optical imaging of intrinsic signals to probe vision in young and adult Bsn<sup>-/-</sup> mice and their wild-type littermates. Here we show that while visual acuity was significantly reduced in mutants compared to controls, vision guided behavioural decisions and optical imaging revealed essentially unperturbed cortical signals and retinotopy in spite of the photoreceptor synaptopathy. In addition, both vision and visual cortical maps were adult-like at 4 weeks of age. These results show that (i) while Bassoon-dependent fast exocytosis is essential for normal vision surprisingly good visual performance can be achieved in the absence of synaptic ribbons, (ii) both the development and maintenance of visual cortical maps is independent of synaptic ribbons and (iii) visual development in the mutants is completed at 4 weeks of age indicating that later developing ectopic synapses do not affect vision. Thus, the central visual system can make use of slow and weak retinal signals to subserve surprisingly robust vision.

© 2009 Elsevier Inc. All rights reserved.

### Introduction

Knowledge about the capacity of visual areas in the central nervous system to process altered retinal input plays a key role in all efforts trying to restore vision in patients with retinal degeneration. In recent years, a number of reports have described plasticity of retinal neurons in animal models of photoreceptor degeneration (Beltran et al., 2006; Claes et al., 2004; Fisher et al., 2005; Peng et al., 2000; Strettoi and Pignatelli, 2000). Mice mutant for the presynaptic scaffolding protein Bassoon display a striking loss of synaptic ribbons anchored to the active zone of photoreceptor terminals with significantly impaired signal transduction through the retina (Dick et al., 2003). However, nothing is known about the central processing of the perturbed retinal signals in this synaptopathy.

Retinal photoreceptors transmit their signals via a unique type of chemical synapse, the ribbon synapse (Dowling, 1987). It is assumed that the ribbon, a structurally and functionally specialized presynaptic cytomatrix, is responsible for a continuous supply of transmitter vesicles. Bassoon is a presynaptic cytomatrix protein, found at the

active zones of both excitatory and inhibitory synapses in the brain (Altmack et al., 2003; Brandstätter et al., 1999; Richter et al., 1999; tom Dieck et al., 1998). In the retina, Bassoon is a major component of the photoreceptor ribbon synapse (Brandstätter et al., 1999; Dick et al., 2001). In Bsn-mutant mice, less than a fifth of the photoreceptors do possess ribbons at all and these are not anchored to the presynaptic active zones but free-floating in the cytoplasm (Dick et al., 2003).

Functionally, this photoreceptor synaptopathy leads to a severely disturbed signal transfer from photoreceptor to bipolar cells: in electroretinographic recordings, the b-wave was not only severely diminished in amplitude but also slowed down (Dick et al., 2003). Whether Bsn-mutant mice can use these severely perturbed signals for basic visual capabilities and whether the slower and diminished signals are sufficient to activate central visual structures was completely unknown. Since the capacity to use altered retinal input to subserve vision is a prerequisite for all efforts to restore vision in patients with retinal degenerative diseases, we used Bsn-mutant mice as a model system to study the central processing and visual capabilities of animals with severely disturbed retinal processing. We applied both behavioural techniques to analyse visual acuity and contrast sensitivity (Prusky et al., 2004, 2000) and optical imaging of intrinsic signals in the same animals to visualize cortical activity (Cang et al., 2005a; Kalatsky and Stryker, 2003; Lehmann and Löwel, 2008) in

\* Corresponding author. Fax: +49 3641 949 102.

E-mail address: [siegrid.loewel@uni-jena.de](mailto:siegrid.loewel@uni-jena.de) (S. Löwel).

Bsn-mutant mice and their wild-type littermates. Our major questions were (i) How well can Bsn-mutant mice see? (ii) How much activity is transmitted to the cortex? (iii) Do visual cortical maps develop? And, since it was recently reported that in the absence of functional Bassoon, ectopic photoreceptor synapses are formed in the outer nuclear layer of the retina starting at about 4 weeks postnatally (Dick et al., 2003; Specht et al., 2007), (iv) do visual capabilities and cortical maps change after ectopic synapse formation?

## Materials and methods

### Animals

Bassoon mutant mice lacking the central part of the protein encoded by exons 4 and 5 of the *Bsn* gene ( $Bsn^{\Delta Ex4/5}$ , here referred to as  $Bsn^{-/-}$ ) and their littermates ( $Bsn^{+/+}$  and  $Bsn^{+/-}$ ) were raised from heterozygous animals at the Leibniz Institute for Neurobiology in Magdeburg, Germany (Altrock et al., 2003). The mice exhibit a mixed genetic background of C57BL/6J and 129/SvEmsJ strains, which is controlled by using sustained C57BL-backcrossed and 129 inbred mice to breed the heterozygous parents. The mice were between 13 and 148 days of age at the time of the experiments. To analyse the development of visual acuity and contrast sensitivity individual mice were tested from the day of eye opening (between postnatal days 13 and 15) until postnatal day 42. To determine visual acuity and contrast sensitivity, we used two behavioural techniques, the virtual optomotor task (Prusky et al., 2004) and the visual water task (Prusky et al., 2004, 2000; Prusky and Douglas, 2004). Finally, we used optical imaging of intrinsic signals to analyse visual cortical activity maps in the same animals. Experimenters were always blind to the animal's genotype. All animal experiments were performed according to the German Law on the Protection of Animals and the corresponding European Communities Council Directive of November 24, 1986 (86/609/EEC).

### Visual acuity and contrast sensitivity

#### Virtual optomotor system

Visual acuity was assessed using the recently developed virtual-reality optomotor system (Prusky et al., 2004). Briefly, freely moving animals are exposed to moving sine wave gratings of various spatial frequencies and contrasts and will reflexively track the gratings by head movements as long as they can see the gratings. Spatial frequency at full contrast and contrast at six different spatial frequencies were varied by the experimenter until the threshold of tracking was determined. Since only motion in the temporal-to-nasal direction evokes tracking it is possible to measure thresholds and contrast functions for both eyes separately by reversing the direction of the moving gratings (Douglas et al., 2005). The threshold for grating acuity and contrast thresholds at the following six spatial frequencies were measured: 0.031, 0.064, 0.092, 0.103, 0.192, 0.272 cycles/degree (cyc/deg). Contrast sensitivity was calculated at each spatial frequency as a Michelson contrast from the screen luminance  $(\max - \min)/(\max + \min)$  and the reciprocal of the threshold (black mean, 0.22 cd/m<sup>2</sup>; white mean, 152.13 cd/m<sup>2</sup>).

Drift speed was usually fixed at 12°/s. To investigate whether genotype had an effect on temporal resolution, we conducted a separate experiment in which drift speed was decreased or increased at different spatial frequencies until no tracking could be observed any longer. For technical reasons we were not able to measure vision at drift velocities higher than 50°/s, so that our plot is therefore truncated. Measurements were performed at the following spatial frequencies (in cyc/deg): 0.064, 0.103, 0.150, 0.192, 0.272 and 0.400 for wild-type animals and 0.064, 0.103, 0.150, 0.192 and 0.200 for  $Bsn^{-/-}$  mice. Experimenters were blind to the animal's genotype and thresholds were regularly validated independently by more than one observer.

To study the development of visual acuity and contrast sensitivity, individual young mice were tested from the day of eye opening throughout development and the genotype (wild-type =  $Bsn^{+/+}$ , heterozygous =  $Bsn^{+/-}$ , mutant =  $Bsn^{-/-}$ ) was determined after visualizing cortical activity maps.

### Visual water task

As a second method to assess visual acuity and contrast sensitivity in mice, we used the so-called visual water task, a visual discrimination task that is based on reinforcement learning (Prusky et al., 2004, 2000; Prusky and Douglas, 2004). For this task, animals are initially trained to distinguish a low spatial frequency vertical grating (0.086 cyc/deg) from equiluminant grey and then their ability to recognize higher spatial frequencies is tested. The apparatus consists of a trapezoidal-shaped pool with two monitors placed side by side at one end. A midline divider is extended from the wide end into the pool, creating a maze with a stem and two arms. The length of the divider sets the choice point and effective spatial frequency. An escape platform that is invisible to the animals is placed below the monitor on which the grating is projected. The position of the grating and the platform is alternated in a pseudorandom sequence over the training and test trials. Once 90% accuracy is achieved, the discrimination threshold is determined by increasing the spatial frequency of the grating until performance falls below 70% accuracy. The highest spatial frequency at which 70% accuracy is achieved is taken as the maximum visual acuity. To measure visual acuity, both  $Bsn^{+/+}$  ( $n = 10$ ) and  $Bsn^{-/-}$  ( $n = 6$ ) were trained and tested in the visual water task. To assess contrast sensitivity contrast thresholds at two different spatial frequencies were measured: 0.086 and 0.201 cycles/degree (cyc/deg) for both  $Bsn^{+/+}$  and  $Bsn^{-/-}$  animals. The contrast of the stimulus grating was decreased in steps of 10% down to 50% contrast, then in steps of 5%.

### Surgical preparations for optical imaging

After initial anaesthesia with 2% halothane in 1:1 O<sub>2</sub>/N<sub>2</sub>O mixture, the animals received an intraperitoneal injection of 50 mg/kg pentobarbital, supplemented by chlorprothixene (0.2 mg/mouse, i.m.), atropine (0.3 mg, s.c.) and dexamethasone (0.2 mg/mouse, s.c.). In addition, lidocaine (2% xylocain jelly) was applied locally to all incisions. A tracheotomy was performed and the animals were placed in a stereotaxic apparatus. Anaesthesia was maintained with 0.6–0.8% halothane in a mixture of 1:1 O<sub>2</sub>/N<sub>2</sub>O applied through the tracheal tube. Body temperature was maintained at 37 °C and electrocardiographic leads were attached to monitor the heart rate continuously throughout the experiment. A craniotomy was prepared over the visual cortex of the left hemisphere. Low melting point agarose (2.5% in saline) and a glass coverslip were placed over the exposed area.

### Optical imaging of intrinsic signals and visual stimuli

Mouse visual cortical responses were recorded using the imaging method developed by Kalatsky and Stryker (2003). In this method, a temporally periodic stimulus is continuously presented to the animal and the cortical response at the stimulus frequency is extracted by Fourier analysis. Briefly, optical images of cortical intrinsic signals were obtained using a Dalsa® 1 M30 CCD camera (Dalsa®, Waterloo, Canada) controlled by custom software. Using a 135 mm × 50 mm tandem lens configuration (Nikon®, Inc., Melville, NY), we imaged a cortical area of 4.6 × 4.6 mm<sup>2</sup>. The surface vascular pattern and intrinsic signal images were visualized with illumination wavelengths set by a green (550 ± 2 nm) or red (610 ± 2 nm) interference filter, respectively. After acquisition of a surface image, the camera was focused 600 μm below the pial surface. An additional red filter was interposed between the brain and the CCD camera. Frames were acquired at a rate of 30 Hz temporally binned to 7.5 Hz and stored as 512 × 512 pixel images after spatial binning of the camera image.

To display visual stimuli, a high refresh rate monitor (Dell® D2128-TCO, 800×600 at 120 Hz) was placed in the right visual field of the animal at a distance of 25 cm to optimally stimulate the right eye (contralateral to the recorded hemisphere). Drifting horizontal or vertical bars were generated by a Matrox G450 board (Matrox Graphics®, Inc., Quebec, Canada), controlled by custom software. The drifting bars were shown across the full screen and were 2° wide, corresponding to a spatial frequency of 0.25 cyc/deg. In some additional experiments, a 1° wide bar, corresponding to a spatial frequency of 0.50 cyc/deg, was used. Visual cortical activity levels (see below) were similar with both stimuli. The distance between two bars was 80° and they were presented at a temporal frequency of 0.125 Hz. For the measurement of contrast sensitivity the contrast of the stimulus bar was reduced stepwise by 5% or 10%.

#### Data analysis

Maps were calculated from the acquired frames by Fourier analysis to extract the signal at the stimulation frequency using custom software (Kalatsky and Stryker, 2003). While the phase component of the signal is used for the calculation of retinotopy, the amplitude component represents the intensity of neuronal activation (expressed as fractional change in reflectance  $\times 10^{-4}$ ). To assess the quality of retinotopic maps, we used the calculation introduced by Cang et al. (2005b). Both the elevation and azimuth maps were used to select the most responsive 20,000 pixels in the visual cortex. For each of these pixels, the difference between its position and the mean position of its surrounding 25 pixels was calculated. For maps of high quality, the position differences are quite small because of smooth progression. The standard deviation of the position difference was then used as an index of the quality of retinotopic maps with small values indicating high map quality and high values indicating low map quality (Cang et al., 2005b). To calculate map area, magnitude maps were thresholded at 30% of peak amplitude, and the area of all selected pixels (1 pixel =  $7.9 \times 10^{-5}$  mm<sup>2</sup>) was summed up. The maximum cortical responses to visual stimuli of different contrasts (Fig. 4) were fitted by a 2nd order polynomial curve.

#### Statistical analyses

All inter-group comparisons were done by Student's two-tailed *t*-test. In analyses in which a within-subject factor was present (i.e., age or spatial frequency), a two-way ANOVA with repeated measurements was performed. The levels of significance were set as \**p*<0.05, \*\**p*<0.01 and \*\*\**p*<0.001. Data are represented as means  $\pm$  s.e.m.

## Results

#### Visual acuity

##### Optometry

The visual acuity of wild-type Bsn+/+ animals (age 70 to 148 days) was  $0.39 \pm 0.003$  cyc/deg in the left and  $0.39 \pm 0.004$  cyc/deg in the right eye. In contrast, visual acuity of Bsn-mutant mice (age 50 to 121 days) was  $0.22 \pm 0.001$  cyc/deg in the left eye and  $0.22 \pm 0.002$  cyc/deg in the right eye. Since there were no differences between values of left and right eyes for both Bsn-/- and Bsn+/+ animals (*t*-test, *p*>0.05 for both comparisons), we averaged values across eyes for both genotypes. Average visual acuity of wild-type Bsn+/+ mice was  $0.39 \pm 0.003$  cyc/deg (*n*=21) compared to  $0.22 \pm 0.001$  cyc/deg (*n*=21) in the mutant Bsn-/- animals (Fig. 1A). Visual acuity of Bsn+/+ mice was thus similar as previously described for C57Bl/6 wild-type mice (Prusky et al., 2004). The difference in visual acuity between Bsn+/+ and Bsn-/- mice was highly significant (*t*-test, *p*<0.001).

#### Visual water task

We trained two groups of mice (Bsn+/+ and Bsn-/-) in the visual water task (Prusky et al., 2000), a cortex-dependent paradigm of visual discrimination learning, to assess their visual acuity (age 60 to 220 days). Visual acuity of Bsn-/- mice was  $0.37 \pm 0.03$  cyc/deg (*n*=6) compared to  $0.56 \pm 0.04$  cyc/deg (*n*=10) in the littermate controls (Bsn+/+) (Fig. 1A). Thus, Bsn-/- mice reached 2/3 of the visual acuity values of their wild-type littermates in this visual discrimination task. The difference in visual acuity between Bsn+/+ and Bsn-/- mice was highly significant (*t*-test, *p*<0.01). While the absolute values of visual acuity in the visual water task were thus higher than those measured in the virtual-reality optomotor system for both genotypes, the difference between Bsn-/- and Bsn+/+ mice was similar in both behavioural tasks: 0.19 cyc/deg in the visual water task and 0.17 cyc/deg in the optomotor system (compare left and right of Fig. 1A). It was recently described also for C57Bl/6 mice that visual acuity measured in the visual water task is consistently higher than in the optomotor task (VWT: 0.5–0.6 cyc/deg (Prusky et al., 2000), optometry: 0.4 cyc/deg (Prusky et al., 2004)).

#### Contrast sensitivity

##### Optometry

Fig. 1B shows contrast sensitivity values of Bsn-/- and Bsn+/+ mice, measured in the optomotor setup and plotted as a function of spatial frequency. Contrast sensitivity of Bsn+/+ mice was clearly superior to the performance of the mutants. Statistical analyses confirmed that genotype had an impact on contrast sensitivity that was highly significant (ANOVA,  $F_{1,49} = 396.59$ , *p*<0.001): For instance, at a spatial frequency of 0.064 cyc/deg Bsn-/- mice had a contrast sensitivity of  $2.9 \pm 0.03$  (corresponding to 35% contrast, *n*=21), while Bsn+/+ littermates had a contrast sensitivity of  $16.3 \pm 0.8$  (or 6% contrast, *n*=21). At a spatial frequency of 0.031 cyc/deg, the contrast sensitivity values for Bsn-/- mice and Bsn+/+ littermates were  $1.8 \pm 0.04$  (corresponding to 59% contrast, *n*=21) and  $3.9 \pm 0.07$  (or 26% contrast, *n*=21), respectively. Thus, contrast sensitivity in Bsn-/- mice was reduced by a factor of 2 to 6 (at the different spatial frequencies) compared to Bsn+/+ littermates indicating that Bsn-/- mice need 2- to 6-fold higher contrasts of visual stimuli to trigger the optomotor reflex. Contrast sensitivity curves peaked at a spatial frequency of 0.064 cyc/deg for both Bsn-/- and Bsn+/+, as previously described for C57Bl/6 mice (Prusky et al., 2004) (Fig. 1B). The contrast sensitivity in wild-type animals was highly significantly different between all spatial frequencies (ANOVA, *p*<0.001 for all comparisons), except between 0.031 and 0.272 cyc/deg. In mutant animals, contrast sensitivity values were highly significantly different between all spatial frequencies (ANOVA, *p*<0.001 for all comparisons), with the exceptions of 0.031 vs. 0.192 cyc/deg and 0.064 vs. 0.092 cyc/deg.

#### Visual water task

The contrast sensitivity of wild-type and mutant animals was also tested in the visual water task at two different spatial frequencies (0.086 and 0.201 cyc/deg). The results of the wild-type animals ( $23.8 \pm 2.39$  at 0.086 cyc/deg and  $20.0 \pm 0.00$  at 0.201 cyc/deg) were in line with values of C57Bl/6 mice as published by Prusky and Douglas (2004). Interestingly, the only Bsn-/- mouse that managed to learn the task had a similar contrast sensitivity as the wild-types. This surprising result is confirmed by a similar result in cortex-dependent contrast sensitivity measurements using optical imaging (see further down).

#### Visual temporal resolution

To test whether the visual deficit of the Bsn-/- mice lies more in the spatial or in the temporal domain, we tested – for a given spatial

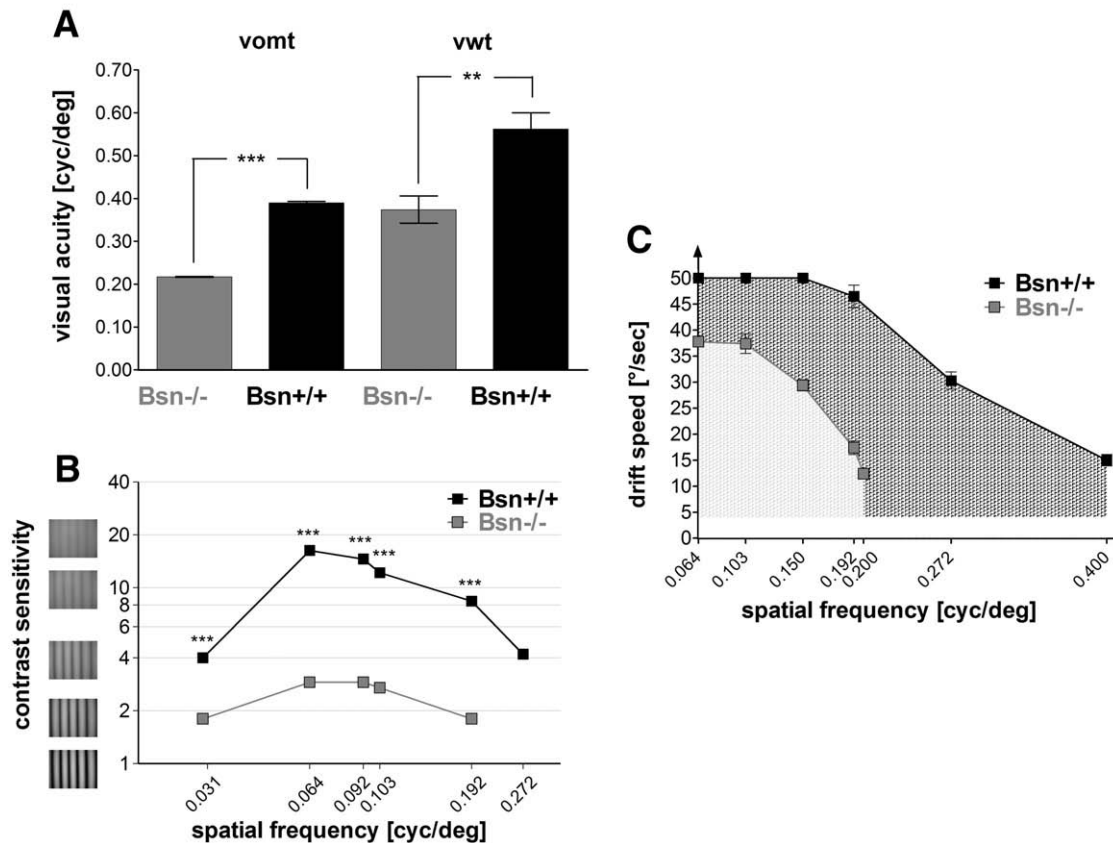


**Fig. 1.** Visual acuity, contrast sensitivity and temporal sensitivity of Bsn<sup>+/+</sup> and Bsn<sup>-/-</sup> mice measured with both the virtual optomotor system and the visual water task. (A) Left: Visual acuity of Bsn<sup>+/+</sup> mice was  $0.39 \pm 0.003$  cyc/deg ( $n = 21$ ) compared to  $0.22 \pm 0.001$  cyc/deg ( $n = 21$ ) in Bsn<sup>-/-</sup> mice in the virtual-reality optomotor task (vomt). The difference in visual acuity was statistically significant ( $t$ -test,  $p < 0.001$ ). Right: Visual acuity of Bsn<sup>+/+</sup> and Bsn<sup>-/-</sup> mice measured with the visual water task (vwt). Visual acuity of Bsn<sup>+/+</sup> mice was  $0.56 \pm 0.04$  cyc/deg ( $n = 10$ ) compared to  $0.37 \pm 0.03$  cyc/deg ( $n = 6$ ) in Bsn<sup>-/-</sup> mice. The difference in visual acuity was statistically significant ( $t$ -test,  $p < 0.01$ ). The difference in visual acuity between Bsn<sup>-/-</sup> and Bsn<sup>+/+</sup> mice is similar in both behavioural tasks: 0.17 cyc/deg in the optomotor system and 0.19 cyc/deg in the visual water task. (B) Contrast sensitivity of Bsn<sup>+/+</sup> ( $n = 21$ ) and Bsn<sup>-/-</sup> animals ( $n = 21$ ) at six different spatial frequencies. Contrast sensitivity of Bsn<sup>-/-</sup> mice was reduced by a factor of 2 to 6 compared to their Bsn<sup>+/+</sup> littermates. Maximal contrast sensitivity was  $2.9 \pm 0.8$  (corresponding to 35% contrast) in Bsn<sup>-/-</sup> compared to  $16.3 \pm 0.03$  (corresponding to 6% contrast) in Bsn<sup>+/+</sup> mice at the spatial frequency of 0.064 cyc/deg. At all spatial frequencies, contrast sensitivity was significantly different between the two genotypes ( $t$ -test,  $p < 0.001$  for all comparisons). (C) Temporal resolution in the optomotor system plotted as a function of spatial frequency. Wild-type ( $n = 4$ ) and mutant ( $n = 5$ ) animals started to respond at drift speeds of about 3°/s. At the spatial frequencies of 0.064, 0.103 and 0.150 cyc/deg, all Bsn<sup>+/+</sup> mice showed tracking up to a drift speed of 50°/s. For technical reasons, we were not able to measure vision at drift velocities higher than 50°/s, so that our plot is therefore truncated. With increasing spatial frequency the highest stimulus velocity at which tracking could be observed decreased to 15°/s at 0.40 cyc/deg. In contrast, Bsn<sup>-/-</sup> mice had lower temporal sensitivities: At a spatial frequency of 0.064 cyc/deg, all Bsn<sup>-/-</sup> mice tracked the moving grating up to a speed of 38°/s. With increasing spatial frequency the highest stimulus velocity at which tracking could be observed decreased to 12°/s at 0.20 cyc/deg. Temporal sensitivity was highly significantly different between Bsn<sup>+/+</sup> and Bsn<sup>-/-</sup> mice (ANOVA,  $p < 0.001$ ).

frequency – the maximum temporal frequency that still evoked a tracking response in the optomotor system. Bsn<sup>+/+</sup> animals started tracking at a drift velocity of  $3.5 \pm 0.29^\circ/s$  ( $n = 4$ ) at all spatial frequencies (Fig. 1C). At 0.064, 0.103 and 0.150 cyc/deg, all Bsn<sup>+/+</sup> mice showed tracking at 50°/s, which is the technical speed limit of our system. With increasing spatial frequency, starting at a spatial frequency of 0.192 cyc/deg, the highest stimulus velocity at which tracking could be observed decreased ( $F = 137.07$ ,  $p < 0.001$ ). At 0.4 cyc/deg, Bsn<sup>+/+</sup> mice tracked stimuli only up to  $15.0 \pm 1.08^\circ/s$ . Bsn<sup>-/-</sup> animals started tracking from a drift speed of  $3.4 \pm 0.25^\circ/s$  ( $n = 5$ ) at all spatial frequencies (Fig. 1C), which was not significantly different from the value of 3.5°/s measured in Bsn<sup>+/+</sup> mice ( $p > 0.5$ ,  $t$ -test). The highest drift speed at which Bsn<sup>-/-</sup> mice could track was dependent on spatial frequency ( $F = 83.88$ ,  $p < 0.001$ ) and peaked at  $37.8 \pm 0.80^\circ/s$  for a 0.064 cyc/deg grating. With increasing spatial frequency, the highest stimulus velocity at which tracking could be observed decreased (ANOVA,  $p < 0.001$ ). At the visual acuity limit of 0.200 cyc/deg, the maximum drift speed of Bsn<sup>-/-</sup> mice was  $12.4 \pm 0.81^\circ/s$ . Statistical analyses showed that temporal resolution across spatial frequencies was highly significantly different between Bsn<sup>+/+</sup> and Bsn<sup>-/-</sup> mice ( $F_{1,7} = 639.535$ ,  $p < 0.001$ , ANOVA).

## Development of visual function

### Visual acuity

We followed vision longitudinally in individual young Bsn<sup>-/-</sup> animals ( $n = 6$ ) and their littermates (Bsn<sup>+/-</sup>:  $n = 15$ , Bsn<sup>+/+</sup>:  $n = 16$ ) from the day of eye opening (postnatal days 13–15) throughout visual development (Fig. 2A). Visual acuity development of Bsn<sup>+/+</sup> and Bsn<sup>+/-</sup> mice was nearly identical and will be described first. On postnatal day 13, average grating acuity of Bsn<sup>+/+</sup> and Bsn<sup>+/-</sup> mice was  $0.05 \pm 0.01$  cyc/deg ( $n = 11$ ) and  $0.04 \pm 0.03$  cyc/deg ( $n = 10$ ), respectively (Fig. 2A). Visual acuity increased rapidly over the following 10 days in both genotypes and reached adult values of 0.4 cyc/deg at postnatal day 29: visual acuity was  $0.40 \pm 0.003$  cyc/deg ( $n = 16$ ) in Bsn<sup>+/+</sup> and  $0.40 \pm 0.004$  cyc/deg in Bsn<sup>+/-</sup> animals ( $n = 15$ ). This rapid increase in visual acuity between 2 and 4 weeks postnatally is in line with previous experiments in C57Bl/6 mice (Prusky et al., 2004).

In contrast to Bsn<sup>+/+</sup> and Bsn<sup>+/-</sup> mice, average grating acuity of Bsn<sup>-/-</sup> mice at postnatal day 13 was  $0.02 \pm 0.04$  cyc/deg ( $n = 3$ ) and thus about half of the other two genotypes (Fig. 2A). Visual acuity increased over the following 10 days and reached adult values

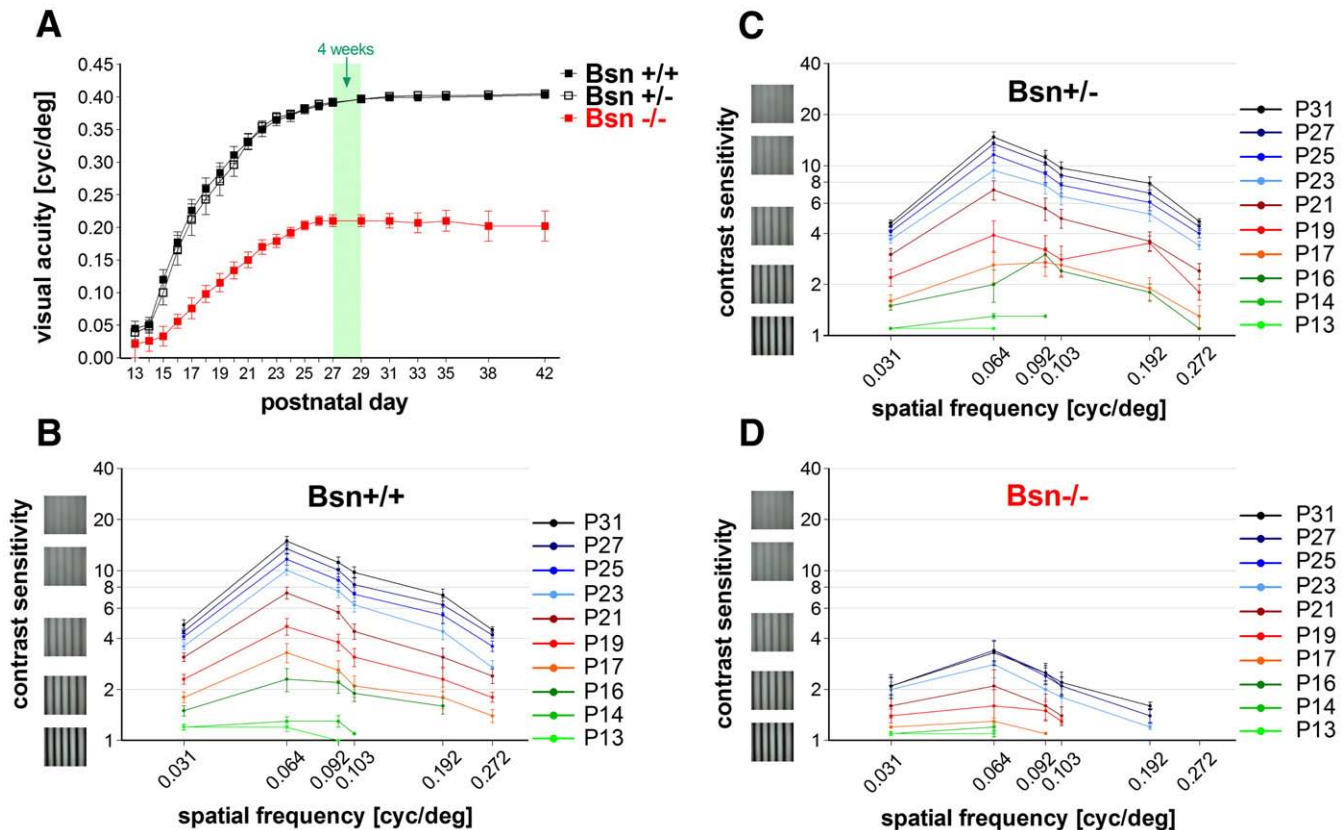


**Fig. 2.** Development of both grating acuity (A) and contrast sensitivity (B–D) from eye opening throughout visual development in Bassoon mutant mice (*Bsn*<sup>-/-</sup>, *n* = 6) and their heterozygous (*Bsn*<sup>+/-</sup>, *n* = 15) and wild-type (*Bsn*<sup>+/+</sup>, *n* = 16) littermates. (A) On postnatal day 13, average visual acuity of both *Bsn*<sup>+/+</sup> and *Bsn*<sup>+/-</sup> mice was 0.04 cyc/deg. Visual acuity increased rapidly over the following 10 days and reached adult values of 0.40 cyc/deg at postnatal day 29. In contrast, average visual acuity of *Bsn*<sup>-/-</sup> mice was only 0.02 cyc/deg on postnatal day 13 but also increased rapidly during the following 10 days and reached adult values of 0.20 cyc/deg at postnatal day 25. (B–D) Development of contrast sensitivity in *Bsn*<sup>+/+</sup> (B), *Bsn*<sup>+/-</sup> (C) and *Bsn*<sup>-/-</sup> mice (D) studied longitudinally in individual animals from eye opening. Between postnatal days 16 and 17, 0.064 cyc/deg emerged as the spatial frequency with the highest contrast sensitivity and remained at the peak of the curves at all subsequent ages in all three genotypes. Contrast sensitivity increased as the mice aged. (B, D) The development of contrast sensitivity in *Bsn*<sup>+/+</sup> and *Bsn*<sup>+/-</sup> animals is nearly identical: adult-like values are reached at postnatal day 31. (D) In *Bsn*<sup>-/-</sup> mice, contrast sensitivity also increased during development and reached maximal values of 3.5 around postnatal day 26 at 0.064 cyc/deg.

of  $0.20 \pm 0.02$  cyc/deg (*n* = 6) on postnatal day 25. There was little variability in the measures between individual animals on a given day and once acuity reached adult values, there was great measurement consistency and stability for each animal. Visual acuity between *Bsn*<sup>+/+</sup> and *Bsn*<sup>-/-</sup> mice was significantly different already on postnatal day 15 (*t*-test, *p* < 0.01). There was also a significant difference in the development of visual acuity between the two genotypes from postnatal day 13 to 42 (two-way ANOVA, *p* < 0.001,  $F_{2,33} = 30.42$ ).

Taken together, this longitudinal study indicates that the time course of visual acuity development is not altered in *Bsn*<sup>-/-</sup> mice compared to their littermates (*Bsn*<sup>+/+</sup> and *Bsn*<sup>+/-</sup>): while visual acuity is significantly lower in *Bsn*<sup>-/-</sup> mice compared to their littermates, all three genotypes reach adult values between postnatal days 25 and 29.

#### Contrast sensitivity

As described previously for C57Bl/6 mice (Prusky et al., 2004), contrast sensitivity also increased rapidly during the first 2 weeks after eye opening. Already between postnatal days 16 and 17, 0.064 cyc/deg emerged as the spatial frequency with the highest contrast sensitivity and remained at the peak at all subsequent ages in all three genotypes. In *Bsn*<sup>+/+</sup> (Fig. 2B) and *Bsn*<sup>+/-</sup> (Fig. 2C) mice, contrast sensitivity at 0.064 cyc/deg increased from  $1.2 \pm 0.1$  (corresponding to 86% contrast) at postnatal day 13 to a value of  $15.0 \pm 0.7$  (corresponding to 5% contrast, *Bsn*<sup>+/+</sup>; *n* = 16) and from  $1.1 \pm 0.02$  (corresponding to 90% contrast) to a value of  $16.6 \pm 0.9$  (corresponding to 6% contrast,

*Bsn*<sup>+/-</sup>; *n* = 15) at postnatal day 31. In contrast, *Bsn*<sup>-/-</sup> mice (Fig. 2D) did not achieve similarly high values. In *Bsn*<sup>-/-</sup> mice, contrast sensitivity at 0.064 cyc/deg increased from  $1.1 \pm 0.07$  (corresponding to 90% contrast) at postnatal day 13 to a maximum of  $3.5 \pm 0.5$  (corresponding to 29% contrast, *n* = 6) at postnatal day 26.

#### Optical imaging

Mouse visual cortical responses were recorded *in vivo* using the imaging method developed by Kalatsky and Stryker (2003). In our experiments, the visual stimuli consisted of moving horizontal (elevation maps; Figs. 3A–C) and vertical bars (azimuth maps, Figs. 3D–F) in the right visual field.

#### Adult animals

Representative examples of the resulting activity and retinotopic maps of the left visual cortex of both *Bsn*<sup>+/+</sup> and *Bsn*<sup>-/-</sup> mice are illustrated in Fig. 3. Most interestingly, *Bsn*<sup>+/+</sup> (Figs. 3C, F) and *Bsn*<sup>-/-</sup> mice (Figs. 3B, E) had nearly identical maps, indistinguishable in both signal amplitude and quality of retinotopy for both elevation (Figs. 3B, C) and azimuth maps (Figs. 3E, F). This was very surprising given the severely reduced synaptic transmission in the retina of *Bsn*<sup>-/-</sup> animals. To thoroughly compare the optical maps of *Bsn*<sup>+/+</sup> and *Bsn*<sup>-/-</sup> mice, we quantified both the magnitude of the visual cortical responses and the quality of the retinotopic maps according to published protocols (Cang et al., 2005b). After visual stimulation with a moving horizontal bar, the magnitude of the optical

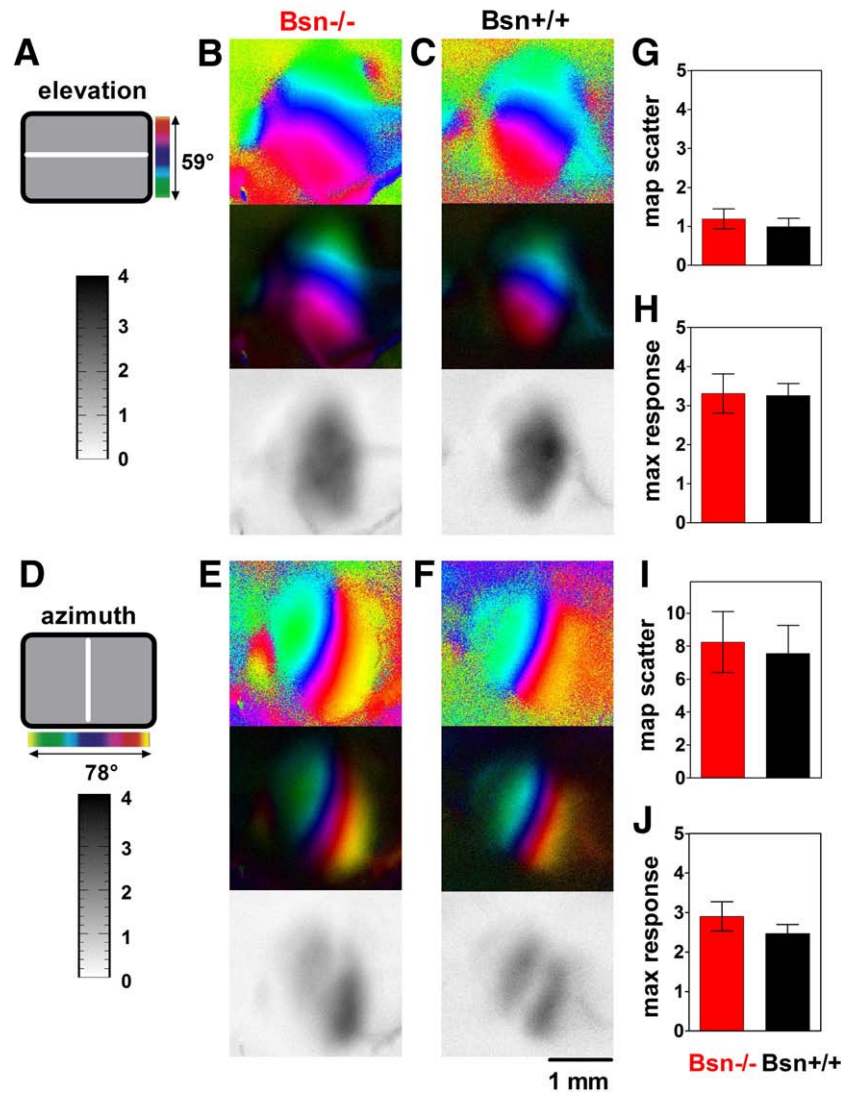


**Fig. 3.** Visual cortical maps recorded with intrinsic signal optical imaging in adult *Bsn+/+* (C, F) and *Bsn-/-* (B, E) mice. Both colour-coded phase and polar maps of retinotopy (top) and grey-scale-coded response magnitude maps (below) and their quantification (G–J) are illustrated. The magnitude of the optical responses is illustrated as fractional change in reflection  $\times 10^{-4}$ . Retinotopic maps are colour-coded according to the schemes on the left side (A, D). Both elevation (B, C) and azimuth (E, F) maps resulting from visual stimulation of the animals with moving horizontal (A) or vertical bars (D) are shown. Note that visual cortical maps of *Bsn-/-* mice have both high response amplitude and excellent retinotopy. (G–J) Quantification of magnitude maps (max. response, H, J) and the quality of retinotopic maps (map scatter, G, I) in both genotypes. Visual cortical maps of *Bsn+/+* ( $n=12$ ) and *Bsn-/-* ( $n=12$ ) animals are indistinguishable in both map quality ( $t$ -test,  $p>0.05$  for elevation,  $p>0.05$  for azimuth maps) and magnitude of the visual cortical responses ( $t$ -test,  $p>0.05$  for elevation,  $p>0.05$  for azimuth maps).

responses in the visual cortex of *Bsn+/+* and *Bsn-/-* mice was nearly identical:  $3.3 \pm 0.3$  ( $n=12$ ) and  $3.3 \pm 0.5$  ( $n=12$ ), respectively (elevation maps; Fig. 3H). The values are statistically not different ( $t$ -test,  $p>0.05$ ). Similarly, after visual stimulation with a moving vertical bar, the magnitude of the cortical responses of *Bsn+/+* and *Bsn-/-* mice was also not significantly different:  $2.5 \pm 0.2$  ( $n=12$ ) in *Bsn+/+* and  $2.9 \pm 0.4$  ( $n=12$ ) in *Bsn-/-* mice (Fig. 3J;  $t$ -test,  $p>0.05$ ).

The quality of the retinotopic maps was also similar in both genotypes. Mean scatter of the elevation maps of *Bsn+/+* mice was  $1.0 \pm 0.2$  ( $n=12$ ) and  $1.2 \pm 0.3$  ( $n=12$ ) in *Bsn-/-* mice (Fig. 3G). For azimuth maps, map scatter was  $7.6 \pm 1.7$  ( $n=12$ ) in *Bsn+/+* mice and  $8.3 \pm 1.9$  ( $n=12$ ) in *Bsn-/-* mice (Fig. 3I). The differences in map scatter were neither significant for elevation ( $t$ -test,  $p>0.05$ ) nor for azimuth maps ( $t$ -test,  $p>0.05$ ).

Finally, there were also no differences in map area between the two genotypes: The cortical region responding to moving horizontal bars (elevation map) was on average  $1.92 \pm 0.119$  mm<sup>2</sup> ( $n=12$ ) for *Bsn+/+* mice and  $1.97 \pm 0.143$  mm<sup>2</sup> ( $n=10$ ) for *Bsn-/-* mice; these sizes were not significantly different ( $t$ -test,  $p>0.05$ ).

To examine the cortical signals also at a high spatial frequency, near the visual acuity limit of the mutant mice, we compared the responses to the usually used  $2^\circ$  wide bar ( $0.25$  cyc/deg) with the responses to a  $1^\circ$  wide bar ( $0.5$  cyc/deg) in some additional experiments. Both visual cortical activity level and map quality were similar with the two types of stimuli. For the  $1^\circ$  stimulus, the magnitude of the optical responses was  $3.2 \pm 0.3$  ( $n=3$ ) and map quality was  $0.9 \pm 0.1$  ( $n=3$ ) and thus not significantly different from the values obtained after visual stimulation with a  $2^\circ$  stimulus ( $t$ -test,  $p>0.05$  for both comparisons).

#### Contrast sensitivity

To have an assessment of contrast sensitivity which is dependent on the visual cortex, we performed additional imaging experiments using visual stimuli of varying contrasts. Fig. 4 illustrates some examples of optical recordings in the visual cortex of wild-type and mutant animals at 100%, 70% and 40% stimulus contrast (Fig. 4A) and their quantification (Fig. 4B). While the maximum response magnitude of the maps generally decreased with decreasing contrast, values

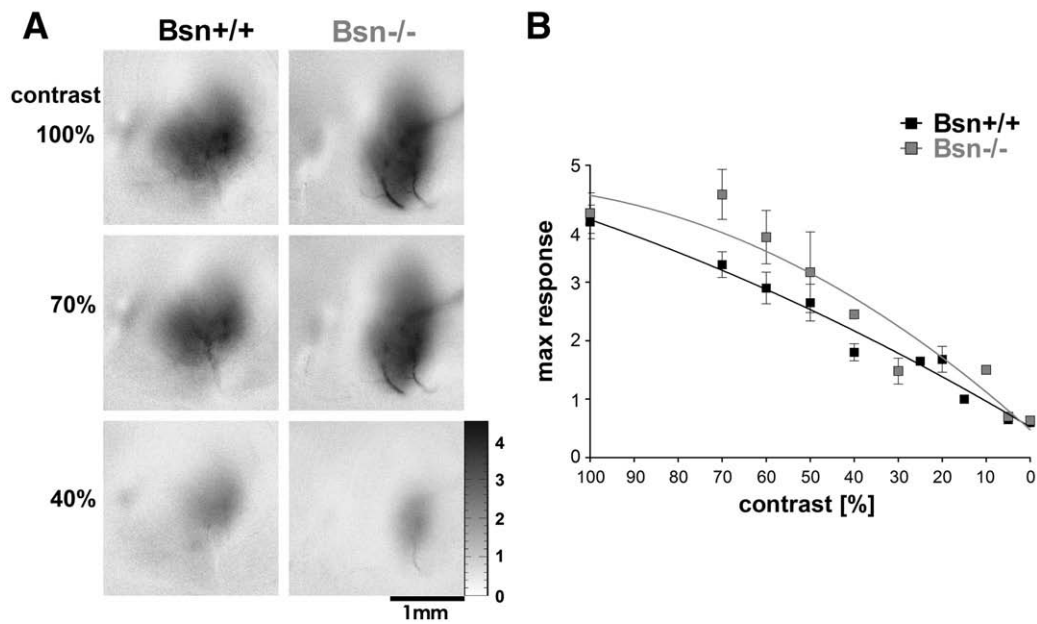


**Fig. 4.** Contrast sensitivity measurements using optical imaging of intrinsic signals in the visual cortex of Bsn+/+ and Bsn-/- mice. (A) Grey-scale-coded response magnitude maps of visual cortical activation of a Bsn+/+ (left column) and a Bsn-/- (right column) mouse induced by a moving horizontal bar (2° wide) of decreasing contrast (100%, 70% and 40%). (B) Maximal cortical responses (mean and standard deviation) plotted as a function of stimulus contrast in wild-type (black squares;  $n=4$ ) and mutant (grey squares;  $n=5$ ) mice. The data were fitted by a 2nd order polynomial curve. Genotypes were not significantly different (ANOVA,  $p>0.05$ ).

were not significantly different between wild-type and Bsn-/- mice (ANOVA,  $p>0.05$ ). This result is in agreement with our contrast sensitivity measurements in the visual water task.

#### Development

To check whether the late developing ectopic synapses in Bsn-/- mice (Dick et al., 2003; Specht et al., 2007) might modify visual cortical maps, we performed optical imaging experiments also in juvenile Bsn-/- animals and compared both signal amplitude and quality of retinotopic maps between juvenile (30 to 49 days of age,  $n=7$ ) and adult animals (81 to 165 days of age,  $n=12$ ). Fig. 5 illustrates an example of a 30-day-old Bsn-/- mouse (Figs. 5C, F), showing that visual cortical maps were adult-like already at this age. Quantitative analyses confirmed this observation and showed that both magnitude of the cortical responses and quality of retinotopic maps were not significantly different between adult and juvenile Bsn-/- animals for both elevation and azimuth maps ( $t$ -test,  $p>0.05$  for all comparisons). The magnitude of the cortical responses for elevation and azimuth maps was  $2.3 \pm 0.3$  and  $2.2 \pm 0.3$  in juvenile Bsn-/- mice and  $3.3 \pm 0.5$  and  $2.9 \pm 0.4$  in adult Bsn-/- mice, respectively (Figs. 5H, J). Mean scatter of the elevation and azimuth maps of juvenile Bsn-/- mice was  $1.65 \pm 0.7$  and  $8.9 \pm 0.7$  and  $1.2 \pm 0.3$  and  $8.3 \pm 1.9$  in adult Bsn-/- mice, respectively (Figs. 5G, I).

#### Discussion

The treatment of patients with retinal degeneration requires fundamental knowledge about the capacity of the retina and of central visual pathways for plasticity and functional remodelling (Jones and Marc, 2005). Plastic changes of retinal neurons in animal models of photoreceptor degeneration were described in a number of studies (Beltran et al., 2006; Claes et al., 2004; Fisher et al., 2005; Peng et al., 2000; Strettoi and Pignatelli, 2000), but a functional interpretation of the changes caused by a mutation were impeded by the rapid degeneration of photoreceptors.

In the present study, we have used Bsn-/- mice that display severely reduced signal transfer from photoreceptors to bipolar cells

(Dick et al., 2003) as a model system to study the central processing and visual capabilities of animals with severely disturbed retinal signals. Visual acuity was significantly reduced in mutants compared to littermate controls and reached adult values already at 4 weeks of age. Interestingly, optical imaging of visual cortical activity (Kalatsky and Stryker, 2003) revealed essentially no differences between Bsn-mutant mice and wild-type littermates. Cortical maps were also adult-like at 4 weeks of age. These results show that (i) robust visual performance can be achieved in the absence of synaptic ribbons, (ii) development and maintenance of visual cortical maps do not depend on synaptic ribbons and (iii) visual development in Bsn-/- mice is completed at 4 weeks of age indicating that later developing ectopic synapses do not seem to contribute to the observed visual capabilities nor improve central visual processing. Thus, the central visual system can make use of slow and weak retinal signals from a severely diseased retina to subservise surprisingly robust vision. Furthermore, the intrinsic optical signal in the visual cortex did not reflect the impairment of the afferent visual signal but must have been amplified either by some intrinsic cortical processing or at some stage of the afferent visual pathway beyond the defective retinal transmission.

Our behavioural tests clearly showed that ribbon-dependent fast exocytosis from photoreceptors is essential for normal visual capabilities. These data confirm previous observations that synaptic ribbons are essential for the precise information processing at photoreceptor synapses as well as at inner ear hair cell synapses, and that, however, active zones without ribbons still retain sufficient functional performance to mediate sensory signal transduction reaching central systems (Dick et al., 2003; Khimich et al., 2005). The possibility that the reduced visual capabilities of the mutants are at least in part due to the function of the Bassoon protein in synapses of the cerebral cortex cannot be excluded (Altrock et al., 2003; Angenstein et al., 2008, 2007).

Photoreceptor cells are nonspiking neurons that use graded changes in membrane potential to transmit sensory information over a wide dynamic range of light intensities. The continuous adjustment of the synaptic output to changes in the incoming signals requires a specialized type of synapse, the ribbon synapse, that sustains high

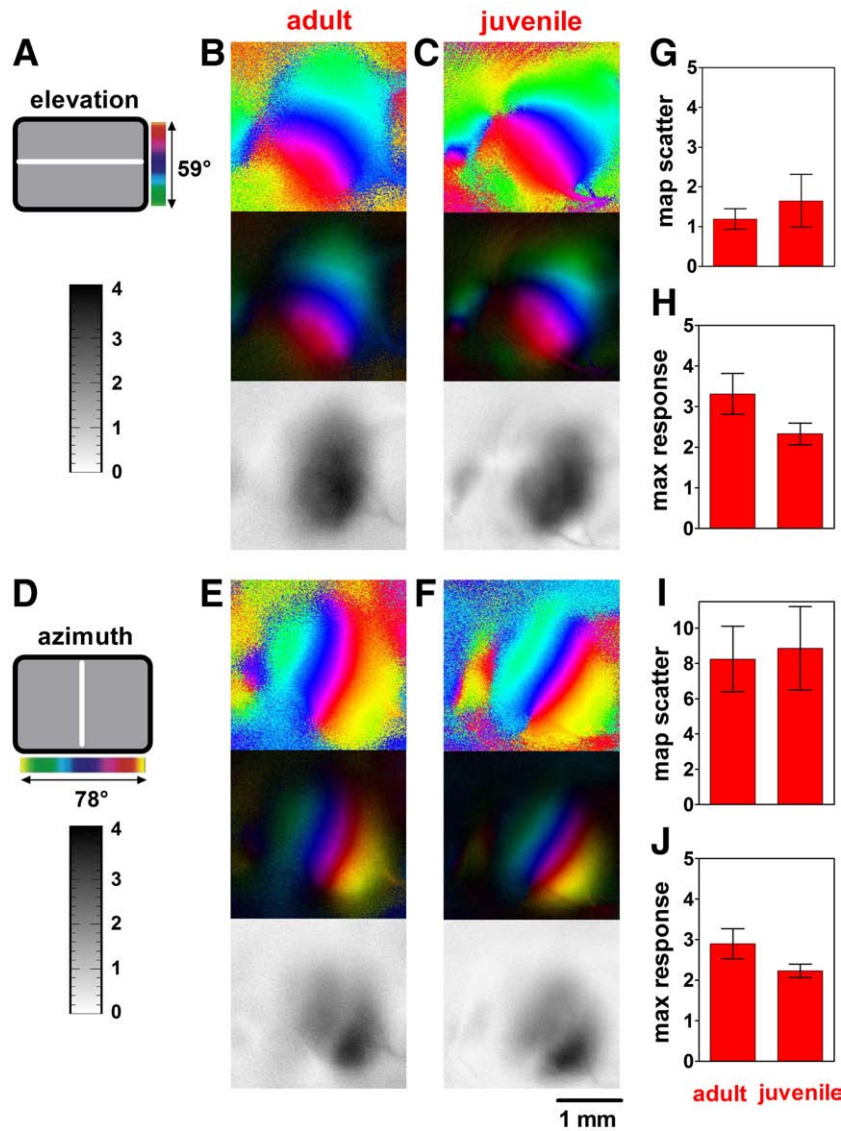


**Fig. 5.** Visual cortical maps recorded with intrinsic signal optical imaging in the visual cortex of an adult (100 days of age; B, E) and a juvenile *Bsn*<sup>-/-</sup> mouse (30 days of age; C, F). Both colour-coded phase and polar maps of retinotopy (top) and grey-scale-coded response magnitude maps (below) and their quantification (G–J) are illustrated. Illustrations and abbreviations as in Fig. 3. Quantitative analyses of the optical imaging data (G–J) demonstrates that visual cortical maps of adult ( $n = 12$ ) and juvenile ( $n = 7$ ) *Bsn*<sup>-/-</sup> mice are indistinguishable in both response magnitude and quality of the retinotopic maps ( $t$ -test,  $p > 0.05$  for all comparisons).

and long-lasting rates of neurotransmitter release (von Gersdorff, 2001; Parsons and Sterling, 2003). In *Bsn*<sup>-/-</sup> mice, neuronal transmission from photoreceptor to bipolar cells is severely impaired. Electroretinographic recordings revealed that the b-wave, which represents activity in second order retinal neurones, was diminished and had a slower time course in *Bsn*<sup>-/-</sup> mice (Dick et al., 2003). While these results showed that there is residual synaptic transmission from photoreceptors to bipolar cells in the retina of *Bsn*<sup>-/-</sup> mice, they provided no information as to whether the remaining neurotransmission is sufficient for the central vision system to get activated nor whether the animals do possess visual capabilities on a behavioural level.

To address these questions, mice were behaviourally tested in two different setups: a virtual-reality optomotor system (Prusky et al., 2004) and a visual water task (Prusky et al., 2000). In addition, visual cortical maps were recorded by optical imaging of intrinsic signals (Kalatsky and Stryker, 2003). While visual acuity of *Bsn*<sup>-/-</sup> mice was reduced compared to *Bsn*<sup>+/+</sup> littermates, the magnitude of visual cortical activation and retinotopic map quality were not altered.

In the visual water task, both *Bsn*<sup>+/+</sup> and *Bsn*<sup>-/-</sup> mice had higher visual acuity than in the optomotor system. This difference was previously observed for C57Bl/6 mice (Prusky et al., 2000) and is most likely due to different neuronal subsystems subserving the behavioural responses in optomotor and reinforcement-based tasks: optokinetic movements are largely driven by subcortical low-frequency visual pathways while grating acuity in the visual water task is driven by cortical circuits (Prusky et al., 2004, 2000; Douglas et al., 2005).

Interestingly, the difference in visual acuity between mutants and controls was identical in the two tasks: *Bsn*<sup>-/-</sup> mice had visual thresholds about 0.2 cyc/deg lower than *Bsn*<sup>+/+</sup> mice. Our results indicate that mice can achieve a visual acuity of about 0.4 cyc/deg even in the absence of proper ribbon synapses and that Bassoon-dependent fast exocytosis is necessary “only” for the additional 0.2 cyc/deg observed in wild-type mice.

The contrast sensitivity of the mutants was especially reduced in the optomotor test, while mutants and wild-type mice performed similarly in the two cortex-dependent assessments, the visual water

task and the optical imaging experiments (Fig. 4), at least for the selected visual stimuli used in these experiments. This interesting result may be explained by a compensation of lost contrast enhancing mechanisms in the retina by contrast enhancing mechanisms in more central parts of the visual system which are not involved in mediating optomotor reflexes. Conversely, the reason for the reduction of contrast sensitivity in the optomotor task in *Bsn*<sup>-/-</sup> mice may be that the retinal signals for the optomotor reflexes are processed by subcortical pathways, so that a loss of contrast enhancing mechanisms in the retina cannot be compensated for by central parts of the visual system. A possible explanation for reduced contrast sensitivity mechanisms in the retina of *Bsn*<sup>-/-</sup> animals may be based on the morphology of the ribbon synapse. In this particular synapse, the postsynaptic dendritic contacts of horizontal cells seem to embrace the anchor site of the ribbons, whereas the contact sites of the bipolar cells are somewhat more distant. This morphology makes it reasonable to assume that a loss of ribbons may affect the synaptic transfer between photoreceptors and horizontal cells more severely than the transfer between photoreceptors and bipolar cells and therefore reduce the efficiency of the inhibitory periphery of the receptive fields. Such a reduction of the inhibitory interactions should result in a reduction of both contrast sensitivity and spatial resolution, as we have indeed observed in our experiments (Figs. 1A, B).

Furthermore, since the range of the inhibitory system is tuned to the optimal spatial frequency, it can be expected that the reduction of contrast sensitivity is largest at this particular spatial frequency. This was also observed in our experiments in the virtual-reality optomotor system: the reduction of contrast sensitivity was largest at the optimal spatial frequency of 0.064 cyc/deg (6 times) and much less (2–5 times) at other spatial frequencies (Fig. 1B). It is therefore possible that contrast enhancing mechanisms in the retina (Kamermans and Spekrijse, 1999) are reduced or switched off while the projection via the bipolar cells is still more or less intact. A reduced input to retinal horizontal cells could also explain the alterations in the b-wave of the electroretinogram in Bassoon mutants (Dick et al., 2003). A reduced and prolonged b-wave could result when the inhibitory system of the horizontal cells is switched off. Thus, missing activity of horizontal cells could account for the reduced amplitude of the b-wave and missing inhibitory interactions could explain its prolonged duration. On the other hand, in both the cortex-dependent visual water task and in the optical imaging experiments contrast sensitivity for the shown visual stimuli was not reduced in *Bsn*-mutant mice compared to their wild-type littermates. Thus, more central stages of visual information processing are obviously able to compensate a loss of lateral inhibition in the retina.

Interestingly, our tests in the optomotor system with different stimulus velocities revealed a significant difference in the temporal sensitivity between wild-type and mutant animals: *Bsn*<sup>-/-</sup> mice tracked grating stimuli up to 38°/s while littermates continued to track the gratings to over 50°/s, the technical speed limit of our system. These results are further evidence for decelerated neuronal processing in the visual pathway of *Bsn*<sup>-/-</sup> mice, presumably at early stages of synaptic processing in the retina, as it is indicated by the prolonged duration of the ERG b-wave (Dick et al., 2003). While the residual synaptic transmission from photoreceptors to bipolar cells is sufficient to mediate basic visual capabilities for *Bsn*<sup>-/-</sup> mice, a deficit becomes obvious when the system is challenged with higher stimulus velocities.

In the absence of functional Bassoon, ectopic photoreceptor synapses are formed in the outer nuclear layer of the retina starting at about 4 weeks postnatally (Dick et al., 2003). By examining mutant retinæ over a period of 2 years, long-lasting plastic changes were observed: ectopic photoreceptor synapses were formed *de novo* by sprouting of both bipolar and horizontal cells resulting in a dense synaptic plexus in the outer nuclear layer, which is absent in wild-type retina (Specht et al., 2007). To check whether ectopic

synapses are responsible for our observations in adult *Bsn*<sup>-/-</sup> mice, we followed vision longitudinally in individual animals from eye opening and also imaged visual cortical maps. These experiments revealed that *Bsn*<sup>-/-</sup> mice reached adult values of both visual acuity and contrast sensitivity at 4 weeks of age and thus before ectopic synapse formation modified retinal structure. In addition, visual cortical maps were adult-like at the same age. It is therefore highly unlikely that the formation and remodelling of ectopic synapses which lasts for at least 1 year (Specht et al., 2007) is responsible for the visual abilities of *Bsn*<sup>-/-</sup> mice or improves vision or central visual processing. It rather indicates that the remaining neuronal transmission of the photoreceptor synapse in mutant mice, i.e., basic exocytosis at ribbon-deficient synapses and additional fusion outside the active zone (Dick et al., 2003; Khimich et al., 2005), is sufficient to sustain decent visual capabilities and activate central visual processing structures.

Taken together, our analyses showed that while Bassoon-dependent fast exocytosis is essential for normal visual capabilities behaviourally relevant visual discrimination was still possible in *Bsn*<sup>-/-</sup> mice. To our knowledge, this is the first study showing that retinal ribbons and proper ribbon attachment at the photoreceptor synapse are not essential for visual discrimination and central visual processing to occur. This observation is very promising for patient studies aiming at restoring at least some function to diseased retinæ because it indicates that even small and slow signals can be sufficient to support vision and prevent central visual structures from disease-related degeneration.

Our results are consistent with a recent report showing that the development of precise retinotopic maps in the visual cortex of mice does not depend on experience-dependent sensory input but is due to waves of spontaneous retinal activity during the first postnatal week. By using a mutant mouse line that has uncorrelated retinal activity during development due to the deletion of the  $\beta$ 2-subunit of the nicotinic acetylcholine receptor, it was demonstrated that the geniculocortical map reaches adult precision by postnatal day 8 and is not further refined by later retinal waves or visual experience (Cang et al., 2005b).

Furthermore, our optical imaging results show that the slower and reduced input signals from the mutant retina into visual cortex are not only sufficient to sustain retinotopic maps but also to activate the cortex as strongly as in normal mice. We take this observation as a strong indication of homeostatic mechanisms (Turrigiano and Nelson, 2004). While it is generally believed that the Hebbian type of network modifications are crucial for shaping cortical circuits as a result of sensory experience, additional homeostatic plasticity may ensure that network compensation can be achieved in response to a wide range of sensory perturbations (Maffei and Turrigiano, 2008; Mrcic-Flogel et al., 2007). We therefore suggest that in *Bsn*<sup>-/-</sup> mice, homeostatic synaptic scaling has adjusted excitatory synaptic strengths of neurons in the afferent visual pathway or in the cortex to compensate for the reductions in activity in the retina.

Overall our results demonstrate that the central visual system has an extraordinarily high potential to process altered inputs from the retina and thus to be instrumental in sustaining behaviourally relevant visual capabilities.

## Acknowledgments

We would like to thank Thomas Dresbach for valuable comments on the manuscript, Katja Krempler, Naira Yeritsyan and Verena Orth for help with some of the experiments, Bettina Kracht for genotyping and supervision of mouse breeding and Anne-Kathrin Pilz and Elke Woker for animal care. Support from the Human Frontier Science Program Grant Award to S.L. and the Deutsche Forschungsgemeinschaft to W.D.A. and E.D.G. is gratefully acknowledged.

## References

- Altmann, W.D., tom Dieck, S., Sokolov, M., Meyer, A.C., Sigler, A., Brakebusch, C., Fässler, R., Richter, K., Boeckers, T.M., Potschka, H., Brandt, C., Löscher, W., Grimberg, D., Dresbach, T., Hempelmann, A., Hassan, H., Balschun, D., Frey, J.U., Brandstätter, J.H., Garner, C.C., Rosenmund, C., Gundelfinger, E.D., 2003. Functional inactivation of a fraction of excitatory synapses in mice deficient for the active zone protein bassoon. *Neuron* 37, 787–800.
- Angenstein, F., Hilfert, L., Zuschratter, W., Altmann, W.D., Niessen, H.G., Gundelfinger, E.D., 2008. Morphological and metabolic changes in the cortex of mice lacking the functional presynaptic active zone protein bassoon: a combined 1H-NMR spectroscopy and histochemical study. *Cereb. Cortex* 18, 890–897.
- Angenstein, F., Niessen, H.G., Goldschmidt, J., Lison, H., Altmann, W.D., Gundelfinger, E.D., Scheich, H., 2007. Manganese-enhanced MRI reveals structural and functional changes in the cortex of Bassoon mutant mice. *Cereb. Cortex* 17, 28–36.
- Beltran, W.A., Hammond, P., Acland, G.M., Aguirre, G.D., 2006. A frameshift mutation in RPRG exon ORF15 causes photoreceptor degeneration and inner retina remodeling in a model of X-linked retinitis pigmentosa. *Invest. Ophthalmol. Vis. Sci.* 47, 1669–1681.
- Brandstätter, J.H., Fletcher, E.L., Garner, C.C., Gundelfinger, E.D., Wässle, H., 1999. Differential expression of the presynaptic cytomatrix protein bassoon among ribbon synapses in the mammalian retina. *Eur. J. Neurosci.* 11, 3683–3693.
- Cang, J., Kalatsky, V.A., Löwel, S., Stryker, M.P., 2005a. Optical imaging of the intrinsic signal as a measure of cortical plasticity in the mouse. *Vis. Neurosci.* 22, 685–691.
- Cang, J., Renteria, R.C., Kaneko, M., Liu, X., Copenhagen, D.R., Stryker, M.P., 2005b. Development of precise maps in visual cortex requires patterned spontaneous activity in the retina. *Neuron* 48, 797–809.
- Claes, E., Seeliger, M., Michalakakis, S., Biel, M., Humphries, P., Haverkamp, S., 2004. Morphological characterization of the retina of the CNGA3(−/−)Rho(−/−) mutant mouse lacking functional cones and rods. *Invest. Ophthalmol. Vis. Sci.* 45, 2039–2048.
- Dick, O., Hack, I., Altmann, W.D., Garner, C.C., Gundelfinger, E.D., Brandstätter, J.H., 2001. Localization of the presynaptic cytomatrix protein Piccolo at ribbon and conventional synapses in the rat retina: comparison with Bassoon. *J. Comp. Neurol.* 439, 224–234.
- Dick, O., tom Dieck, S., Altmann, W.D., Ammermüller, J., Weiler, R., Garner, C.C., Gundelfinger, E.D., Brandstätter, J.H., 2003. The presynaptic active zone protein bassoon is essential for photoreceptor ribbon synapse formation in the retina. *Neuron* 37, 775–786.
- Douglas, R.M., Alam, N.M., Silver, B.D., McGill, T.J., Tschetter, W.W., Prusky, G.T., 2005. Independent visual threshold measurements in the two eyes of freely moving rats and mice using a virtual-reality optokinetic system. *Vis. Neurosci.* 22, 677–684.
- Dowling, J.E., 1987. *The Retina: An Approachable Part of the Brain*. Belknap Press of Harvard University Press, Cambridge.
- Fisher, S.K., Lewis, G.P., Linberg, K.A., Verardo, M.R., 2005. Cellular remodeling in mammalian retina: results from studies of experimental retinal detachment. *Prog. Retin. Eye Res.* 24, 395–431.
- Jones, B.W., Marc, R.E., 2005. Retinal remodeling during retinal degeneration. *Exp. Eye Res.* 81, 123–137.
- Kalatsky, V.A., Stryker, M.P., 2003. New paradigm for optical imaging: temporally encoded maps of intrinsic signal. *Neuron* 38, 529–545.
- Kamerlings, M., Spekreijse, H., 1999. The feedback pathway from horizontal cells to cones. A mini review with a look ahead. *Vision Res.* 39, 2449–2468.
- Khimich, D., Nouvian, R., Pujol, R., tom Dieck, S., Egner, A., Gundelfinger, E.D., Moser, T., 2005. Hair cell synaptic ribbons are essential for synchronous auditory signalling. *Nature* 434, 889–894.
- Lehmann, K., Löwel, S., 2008. Age-dependent ocular dominance plasticity in adult mice. *PLoS ONE* e3120, 3.
- Maffei, A., Turrigiano, G.G., 2008. Multiple modes of network homeostasis in visual cortical layer 2/3. *J. Neurosci.* 28, 4377–4384.
- Mrsic-Flogel, T.D., Hofer, S.B., Ohki, K., Reid, R.C., Bonhoeffer, T., Hübener, M., 2007. Homeostatic regulation of eye-specific responses in visual cortex during ocular dominance plasticity. *Neuron* 54, 961–972.
- Parsons, T.D., Sterling, P., 2003. Synaptic ribbon. Conveyor belt or safety belt? *Neuron* 37, 379–382.
- Peng, Y.W., Hao, Y., Petters, R.M., Wong, F., 2000. Ectopic synaptogenesis in the mammalian retina caused by rod photoreceptor-specific mutations. *Nat. Neurosci.* 3, 1121–1127.
- Prusky, G.T., Douglas, R.M., 2004. Characterization of mouse cortical spatial vision. *Vision Res.* 44, 3411–3418.
- Prusky, G.T., West, P.W., Douglas, R.M., 2000. Behavioral assessment of visual acuity in mice and rats. *Vision Res.* 40, 2201–2209.
- Prusky, G.T., Alam, N.M., Beekman, S., Douglas, R.M., 2004. Rapid quantification of adult and developing mouse spatial vision using a virtual optomotor system. *Invest. Ophthalmol. Vis. Sci.* 45, 4611–4616.
- Richter, K., Langnaese, K., Kreutz, M.R., Olias, G., Zhai, R., Scheich, H., Garner, C.C., Gundelfinger, E.D., 1999. Presynaptic cytomatrix protein bassoon is localized at both excitatory and inhibitory synapses of rat brain. *J. Comp. Neurol.* 408, 437–448.
- Specht, D., tom Dieck, S., Ammermüller, J., Regus-Leidig, H., Gundelfinger, E.D., Brandstätter, J.H., 2007. Structural and functional remodeling in the retina of a mouse with a photoreceptor synaptopathy: plasticity in the rod and degeneration in the cone system. *Eur. J. Neurosci.* 26, 2506–2515.
- Strettoi, E., Pignatelli, V., 2000. Modifications of retinal neurons in a mouse model of retinitis pigmentosa. *Proc. Natl. Acad. Sci. U. S. A.* 97, 11020–11025.
- tom Dieck, S., Sanmarti-Vila, L., Langnaese, K., Richter, K., Kindler, S., Soyke, A., Wex, H., Smalla, K.H., Kämpf, U., Fränzer, J.T., Stumm, M., Garner, C.C., Gundelfinger, E.D., 1998. Bassoon, a novel zinc-finger CAG/glutamine-repeat protein selectively localized at the active zone of presynaptic nerve terminals. *J. Cell. Biol.* 142, 499–509.
- Turrigiano, G.G., Nelson, S.B., 2004. Homeostatic plasticity in the developing nervous system. *Nat. Rev. Neurosci.* 5, 97–107.
- von Gersdorff, H., 2001. Synaptic ribbons: versatile signal transducers. *Neuron* 29, 7–10.